Performance Evaluation of A Single-Phase Three-Port Boost-Rectifier-Based PFC Converter with Stacked/Sigma Configuration for Higher Voltage Step-up Application

Hongfei Wu, Meng Han, Yihang Jia, Yan Xing
Center for More-Electric-Aircraft Power Systems, College of Automation
Nanjing University of Aeronautics and Astronautics
Nanjing, China
Email: wuhongfei@nuaa.edu.cn

***Abstract*—A single-phase three-port Boost-rectifier-based PFC converter with DC-Port stacked/sigma configuration for higher voltage step-up applications is evaluated in this paper. To reduce the voltage stresses and switching losses of the Boost PFC converter, dual DC voltage ports are built using a Boost PFC converter, and a high-efficiency unregulated DC-DC transformer, DCX, is adopted to connect the two DC ports in series. Therefore, higher DC output voltage is achieved with the stacked configuration. Control strategy based on the volt-second balance of the inductor is adopted so that transition between different working modes is realized smoothly. The presented AC-DC converter has the merits of lower voltage stresses and lower switching losses because of the three voltage-levels characteristics of the TPR. Experimental results based on a 2-kW 100-kHz prototype are provided to evaluate the effectiveness and advantage of the analyzed method.**

***Keywords*—AC-DC converter; dual DC voltage ports; stacked configuration; three voltage-levels**

I. INTRODUCTION

The DC output voltage of a single-phase Boost PFC converter is usually designed to be slightly higher than the peak amplitude of AC line voltage to ensure high efficiency and high power factor. For example, the DC output voltage of a 220VAC/50Hz PFC converter is usually in the range of 380V-420VDC [1][2][3]. A higher DC voltage is required for some applications such as single phase to three phase PWM inverter fed motor drive [4] and electric vehicles power systems [5][6]. However, the efficiency of a Boost PFC converter decreases dramatically with the increase of DC output voltage due to the high conduction and switching losses [7][8]. There have been many coupled-inductor-based high step-up Boost converters proposed for DC voltage conversion applications [9][10]. However, these converters are rarely used in single phase PFC applications, because the performance of these converters is affected a lot by the periodically changing AC input voltage. In addition, additional auxiliary circuit is needed to suppress the high voltage spike induced by coupled inductors. In [11][12][13], voltage-doubler technique is introduced to the Boost PFC converter to realize higher voltage step-up. However, the minimum voltage gain of a voltage-doubler Boost converter must be N (N is the number of voltage-doubler in the Boost converter) times of a traditional Boost converter, which makes the DC output voltage cannot be regulated flexibly.

In this paper, a single-phase three-port Boost-rectifier-based PFC converter with two DC output ports and DC-port stacked/sigma configuration is analyzed for higher voltage step-up application. Two DC outputs are generated without increasing the voltage step-up ratio of a traditional Boost PFC converter, and the two DC output are connected in series with the help of a DC transformer, DCX, to realize higher DC output voltage. The analysis indicates that high efficiency and low voltage stresses can be achieved with the presented solutions.

II. TOPOLOGY AND OPERATION PRINCIPLE

A. Topology and analysis

The analyzed sigma PFC converter is shown in Fig. 1. It is constructed with a TPR and an isolated DCX. The TPR, which is realized with a Boost type topology, can provide an AC voltage input, v_{ac}, and dual DC voltage outputs, i.e. V_L and V_H, simultaneously. As shown in Fig. 1, the low voltage V_L is used as the input of the DCX because the voltage stress, power rating and power loss of the DCX are less with this kind of connection method. The output voltage of the DCX V_{Lo} which equals to V_L is in series with the voltage V_H. Therefore, a higher output voltage V_o which equals to the sum of V_{Lo} and V_H can be obtained. Two outer voltage loops are employed to regulate the voltage V_{Lo} and V_H, respectively. Another inner current loop is employed to regulate the inductor current whose magnitude is determined by the sum of v_{mL} and v_{mH}. v_{mL} and v_{mH} are the outputs of the low and high voltage control loop, respectively. Furthermore, a mode switching controller is used to determine the power distribution between the V_L and V_H voltage port.

This work was supported by the National Natural Science Foundation of China (51677085), Grants from the Power Electronics Science and Education Development Program of Delta Environmental & Educational Foundation (DREG2016007), Six talent peaks project in Jiangsu Province (2016-XNYQC-008) and "QingLan" Projiect.

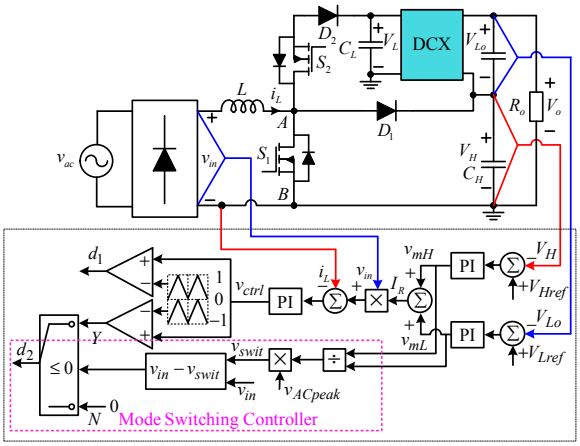

Fig.1. Topology and control block of the evaluated converter

In this paper, a novel control method is applied to the TPR to regulate the voltage V_L and V_H simultaneously. With the analyzed control method, only one power switch is modulated at high frequency to shape the input current while the other one is kept ON or OFF at the frequency of the line voltage to distribute energy between the V_L and V_H voltage ports. For the convenience of analysis, the switching voltage v_{swit} which is smaller than the peak voltage of the input ac voltage v_{ACpeak}, is defined. v_{swit} is definitely smaller than V_H but can be either smaller or higher than V_L. According to the relationship between the voltage v_{swit} and V_L, There are two operation conditions for the analyzed converter.

B. Operational Principle when $v_{swit} \leq V_L$

The key waveforms of the TPR when $v_{swit} \leq V_L$ are shown in Fig. 2. In order to realize smooth mode transition, dual-carrier-based PWM modulation strategy is adopted for the stacked AC-DC converter. As shown in Fig. 2, v_{ctrl} is the modulation waveform i.e. the output signal of the current regulator, and v_{c1}/v_{c2} are the carriers. v_{c1} is biased by the peak amplitude of v_{c2}. The TPR has two operation modes according to the relationship between the rectified input voltage v_{in} and the switching voltage v_{swit}. When $v_{in} < v_{swit}$, the modulation wave v_{ctrl} will be greater than v_{c2}, and the converter works in Mode 1, in which v_{ctrl} only intersects the upper carrier v_{c1}, the switch S_2 keeps in ON-state and the diode D_1 keeps in OFF-state. The equivalent circuit of the Mode 1 is shown in Fig. 3, where a Boost PFC is built by the inductor L, the switch S_1 and the diode D_2. It is obvious that, in the mode 1, all the input power is supplied to the low voltage port V_L.

When $v_{in} > v_{swit}$, the converter works in Mode 2 and the switch S_2 is forced to turn off. The modulation wave will have a step-up change and inserter the carrier v_{C1} again. Therefore, step-up change is happened to D_1 at the boundary of mode switching in order to control the input current tightly. The equivalent circuit of Mode 2 is shown in Fig. 4, where a Boost PFC is built by the inductor L, the switch S_1 and diode D_1. Compared with Mode 1, it can be seen that all the input power is supplied to the high voltage port when the convert works in Mode 2.

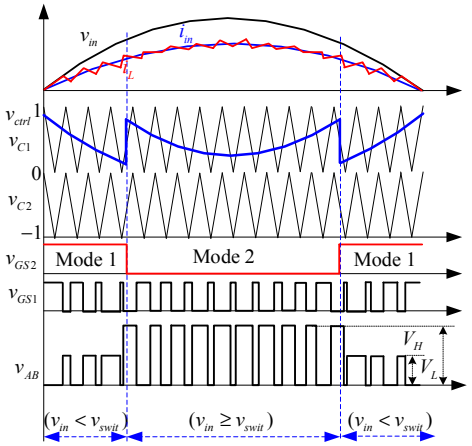

Fig. 2. Key waveforms of the analyzed converter when $v_{swit} \leq V_L$

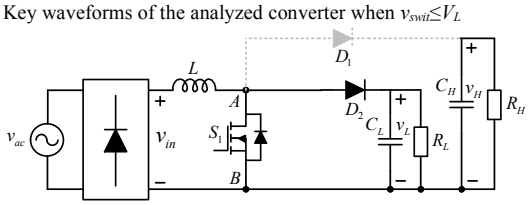

Fig. 3. Equivalent circuit of the Mode 1

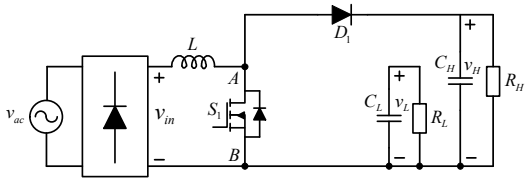

Fig. 4. Equivalent circuit of the Mode 2

According to the working principle of the TPR, it can be seen that the input power is divided into two parts in the scale of half period of the line voltage. When the converter works in Mode 1, i.e. $v_{in} < v_{swit}$, all the input power is supplied to the low voltage port. On the contrary, all the input power is supplied to the high voltage port when $v_{in} > v_{swit}$. As a result, it can be indicated that the voltage v_{swit} can be used as a control variable to regulate the output voltage V_L and V_H, simultaneously.

C. Operational Principle when $v_{swit} > V_L$

It should be noted that when $v_{swit} > V_L$, the converter will enter into another working mode when $v_{in} < v_{swit}$. The key waveforms of the TPR when $v_{swit} > V_L$ are shown in Fig. 5. It can be seen that when $V_L < v_{in} < v_{swit}$, the modulation waveform v_{ctrl} will be lower than v_{c1} and the converter operates in Mode 3, in which v_{ctrl} only intersects with the lower carrier v_{C2} and the switch S_1 is in OFF-state. The equivalent circuit of Mode 3 is shown in Fig. 6(a). The switch S_2 is modulated at high frequency to shape the input current. As shown in Fig. 6(b), when S_2 is ON, the inductor is charged by the voltage difference v_{in}-V_L and the input power is supplied to the low voltage port V_L. As shown in Fig. 6(c), when S_2 is OFF, the inductor is discharged and the input power is supplied to the high voltage port V_H. Different from Mode 1 and Mode 2, the input energy is supplied to the V_L and V_H port alternatively in

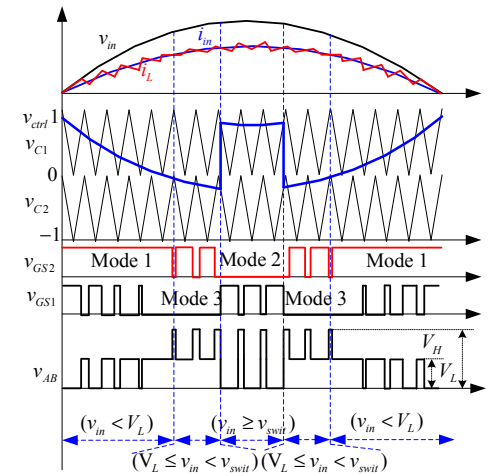

Fig. 5. Key waveforms of the analyzed converter when $v_{swit}>V_L$

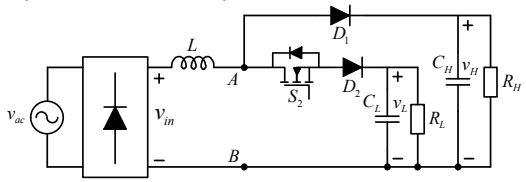

(a) Equivalent circuit of the Mode 3

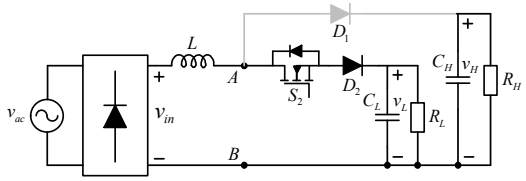

(b) Equivalent circuit when S_2 is ON

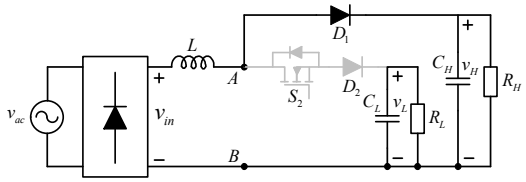

(c) Equivalent circuit when S_2 is OFF

Fig. 6. Equivalent circuit of the Mode 3

the switching period with the switch S_2 ON and OFF when the converter works in Mode 3.

D. Characterization

1) *Power ratio versus normalized switching voltage v_{swit}/v_{ACpeak}*

According to the working principals of the converter, the switching voltage v_{swit} and the operation mode determine the power supplied to the V_L port essentially. Supposing the power converter is lossless and harmonic free, the instantaneous ac input power can be calculated as

$$p_{in}(t) = v_{in}(t) i_{in}(t) = \frac{V_{ACpeak} I_{ACpeak}}{2}(1-\cos 2\omega t) \tag{1}$$

where V_{ACpeak} and I_{ACpeak} are the peak values of the input voltage and current, respectively. As shown in Fig. 3, when the TPR works in Mode 1, all the input power is supplied to the V_L port and it can be found as

$$p_{L\_Mode1} = p_{in} = \frac{V_{ACpeak} I_{ACpeak}}{2}(1-\cos 2\omega t) \tag{2}$$

On the contrary, all the input power is consumed by the V_H port and thus

$$p_{L\_Mode2} = 0 \tag{3}$$

However, when the TPR works in Mode 3, the input power will be supplied to the V_L and V_H port alternatively in the switching period. As shown in Fig. 6(b), the input power is transformed to the V_L port when S_2 is ON. Therefore, the instantaneous power transformed to the V_L port in Mode 3 can be obtained as

$$p_{L\_Mode3} = I_m \sin \omega t \cdot d_2 \cdot V_L \tag{4}$$

When $v_{swit} \leq V_L$, the TPR works between Mode 1 and Mode 2. Therefore, the average power consumed by the V_L port can be calculated as

$$P_L = \frac{2}{\pi}\int_0^{\arcsin(v_{swit}/V_m)} p_{L\_Mode1}\, d\omega t \tag{5}$$

Then the power ratio of the V_L and V_H port can be expressed as

$$P_L/P_H = \frac{2\arcsin\frac{v_{swit}}{v_{ACpeak}} - \sin(2\arcsin\frac{v_{swit}}{v_{ACpeak}})}{\pi - 2\arcsin\frac{v_{swit}}{v_{ACpeak}} + \sin(2\arcsin\frac{v_{swit}}{v_{ACpeak}})} \tag{6}$$

By defining the normalized switching voltage $k=v_{swit}/v_{ACpeak}$, the equation (6) can be further simplified as

$$P_L/P_H = \frac{2\arcsin(k) - \sin(2\arcsin(k))}{\pi - 2\arcsin(k) + \sin(2\arcsin(k))} \quad 0 \leq k \leq V_L/v_{ACpeak} \tag{7}$$

It can be seen that when $v_{swit} \leq V_L$, power ratio P_L/P_H is only determined by the normalized voltage k.

When $v_{swit}>V_L$, the TPR will work into Mode 3 on the condition that $V_L<v_{in}<v_{swit}$. Therefore, the average power consumed by the V_L port can be calculated as

$$P_L = \frac{2}{\pi}\int_0^{\arcsin(V_L/V_m)} p_{L\_Mode1}\, d\omega t + \frac{2}{\pi}\int_{\arcsin(V_L/V_m)}^{\arcsin(v_{swit}/V_m)} p_{L\_Mode3}\, d\omega t \tag{8}$$

Then the power ratio P_L/P_H when $v_{swit}>V_L$ can be calculated as

$$P_L/P_H = \frac{\beta}{\pi V_m (V_H - V_L) - \beta} \quad 0 \leq k \leq V_L/v_{ACpeak} \tag{9}$$

where β can be expressed as

$$\begin{aligned}\beta = {} & 2V_H V_L \sqrt{1-\frac{V_L^2}{V_m^2}} + 2V_H V_m \arcsin\frac{V_L}{V_m} - 2V_L V_m \arcsin k \\ & - 2V_L\sqrt{1-k^2}(2V_H - kV_m)\end{aligned} \tag{10}$$

It can be seen that the power ratio P_L/P_H is concerned with the voltage v_{ACpeak}, V_L and V_H. Fig. 7 shows the curve of P_L/P_H with respect to v_{swit}/v_{ACpeak}, at different peak ac voltage v_{ACpeak} when V_L=250V and V_H=400V. Since the two DC output ports of the TPR are in series connection, P_L/P_H equals to V_L/V_H. Therefore, a theoretical value of v_{swit} can also be found from the curves shown in Fig. 7.

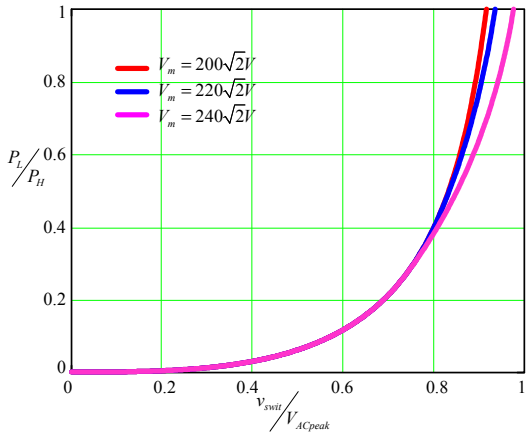

Fig. 7. Power Ratio versus normalized switching voltage

2) *Duty ratio analysis*

Based on the volt-second balance of the inductor L and the control logic of the mode switching controller, the duty ratio of S_1 and S_2, i.e. d_1 and d_2 can be expressed as follows:

$$d_1(t)=\begin{cases}1-\dfrac{v_{in}}{V_L} & \text{Mode 1}\\ 1-\dfrac{v_{in}}{V_H} & \text{Mode 2}\\ 0 & \text{Mode 3}\end{cases} \tag{11}$$

$$d_2(\mathrm{t})=\begin{cases}1 & \text{Mode 1}\\ 0 & \text{Mode 2}\\ 1-\dfrac{v_{in}-V_L}{V_H-V_L} & \text{Mode 3}\end{cases} \tag{12}$$

Fig. 8 shows the curves of d_1 and d_2 when v_{ac}=220VAC, V_H=400V and V_L=300V/180V. As shown in Fig. 8(a), when V_L=300V, the converter works in Mode 1 and Mode 2. The duty ratio d_2 equals to be 1 in Mode 1 while equals to 0 in Mode 2. It can be seen that S_2 works as a low-frequency switch to determine which voltage port is charged by the input power. As shown in Fig. 8(a), the switch S_1 works at high-frequency to shape the inductor current and a step change occurs at the boundary of Mode 1 and Mode 2. Based on the volt-second balance of the inductor L, the initial value of d_1, i.e. d_{1_Mode2} when the TPR enters into Mode 2 and the last value of d_1, i.e. d_{1_Mode1} when the TPR works in Mode 1 should satisfy

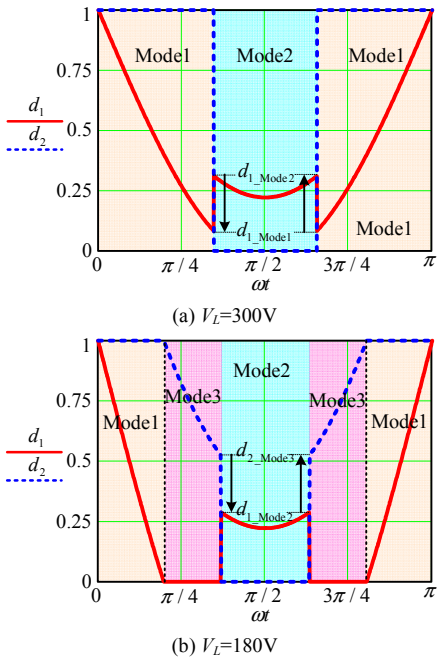

Fig. 8. Curves of d_1 and d_2

$$d_{1\_Mode2}=\frac{V_H-V_L}{V_H}+\frac{V_L}{V_H}d_{1\_Mode1} \tag{13}$$

According to (13), a predicted initial value can be calculated and added to the modulation wave when the TPR enters into Mode 2. Similarly, a step-down initial value can also be pre-added to the modulation wave when the TPR switches back to Mode 1 from Mode 2. Therefore, a smooth transition between Mode 1 and Mode 2 can also be realized.

As shown in Fig. 8(b), when V_L=180V, the TPR will enter into Mode 3 in which d_1 reaches to zero and d_2 is modulated to regulate the inductor current. It can be seen that the transition between Mode 1 and Mode 3 is naturally smooth. Similarly to the curves shown in Fig. 8(a), step changes occur at the boundary of Mode 2 and Mode 3 and the duty ratio d_{2_Mode3} and d_{1_Mode2} should satisfy

$$d_{1\_Mode2}=\frac{V_H-V_L}{V_H}d_{2\_Mode3} \tag{14}$$

Based on (14), a predicted value can be calculated and added to the modulation waveform to realize the smooth transition between Mode 2 and Mode 3.

III. Simulation And Experimental Verification

In order to evaluate the operation of the analyzed sigma AC-DC converter, simulation is carried out using Power Simulation (PSIM) software. The topology is shown in Fig. 1. The input voltage of the TPR converter is 220VAC±20%AC, the low voltage port V_L is 250V, the high voltage port is 400V, the output voltage is 650V, and the rated power of the AC-DC converter is 2kW.

Fig. 9 shows the simulation steady-state waveforms of the TPR at full load with v_{ac}=264VAC. It can be seen that the TPR works among Mode 1, Mode 2 and Mode 3 in half period of the input voltage. Therefore, as shown in Fig. 9(b), the pole voltage v_{AB} changes among three voltage levels, i.e. 0, V_L and V_H. v_{Lb} is the voltage across the inductor L. It should be noted that the switching losses of the analyzed converter can be reduced significantly because only one switch is operated at high frequency and three voltage-levels characteristic can be obtained by the TPR.

The simulation steady-state waveforms of V_L, V_H, line voltage v_{ac} and line current i_{ac} are shown in Fig. 10. It is seen that the line current is in phase with the line voltage. The lower voltage port V_L is lower than the peak amplitude of the line voltage v_{ac}, while the high voltage port V_H, which is equivalent to the output voltage of the front-end PFC converter in two-stage AC/DC converter, is higher than the peak line voltage.

To verify the analysis, a 2kW 100-kHz prototype is established. The input AC voltage v_{AC}=220V±20%AC/50Hz and the output load voltage V_o=650V. The DCX is implemented using the open-loop operated soft-switching LLC resonant converter with unit gain. The LLC converter is always operated at its resonant frequency f_r=100kHz. The high voltage V_H and low voltage V_L of the TPR are designed to be 400V and 250V, respectively. The parameters of the TPR are as follows. S_1/S_2: IPW60R070C6, D_1/D_2: HFA30PA60CPbF, L: 300uH, C_L: 1470uF, C_H: 940uF.

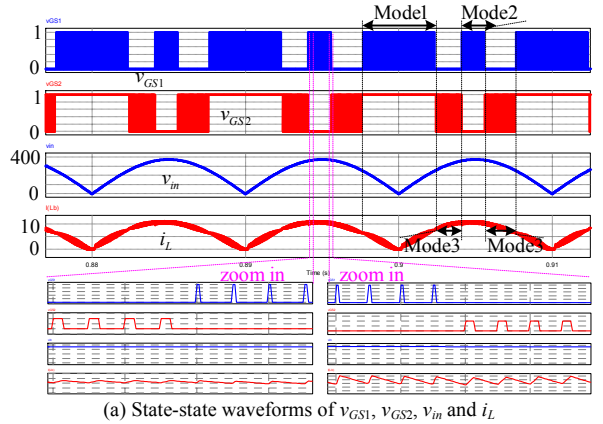

(a) State-state waveforms of v_{GS1}, v_{GS2}, v_{in} and i_L

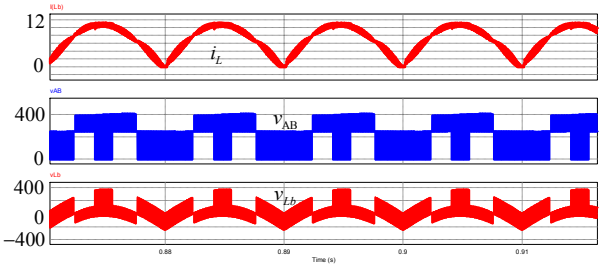

(b) State-state waveforms of i_L, v_{AB}, and v_L

Fig. 9. Steady-state simulation waveforms with v_{ac}=264VAC

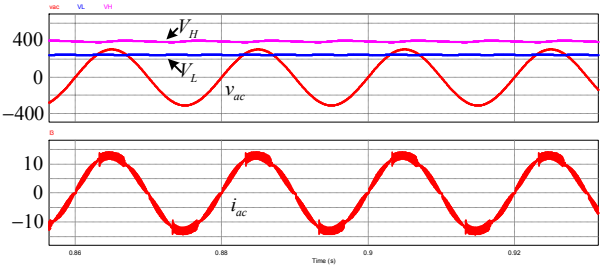

Fig. 10. State-state simulation waveforms of V_H, V_L, v_{ac} and i_{ac} with v_{ac}=220VAC

Fig. 11(a) shows the steady-state waveforms of the TPR at full load with v_{ac}=180VAC. v_{GS1} and v_{GS2} are the driving voltage of switches S_1 and S_2. The converter works between Mode 1 and Mode 2. It can be seen that the inductor current i_L is well regulated in the two operation modes. As shown in Fig. 11(b) and Fig. 11(c), the duty ratio of S_1 has a step-up and step-down change at the boundary of the mode switching. The inductor current is controlled tightly and the mode switching is smooth.

Fig. 12 shows the dynamic waveforms of the analyzed sigma AC-DC converter with the load stepping up from 50% of full load to full load. It can be seen that the voltage V_L, V_H, V_o and the input ac current i_{ac} are well regulated when the load steps up. The overall efficiency of the analyzed converter is shown in Fig. 13. It can be seen that higher efficiency is obtained with the analyzed TPR PFC converter based on the DC-port stacked configuration due to the reduced voltage stresses and switching losses. Fig. 14 shows the losses of the front-end TPR and the LLC-DCX, respectively. It can be seen that losses of the DCX is much lower than that of TPR because

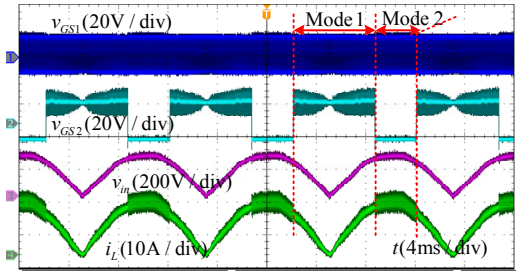

(a) Overall waveforms

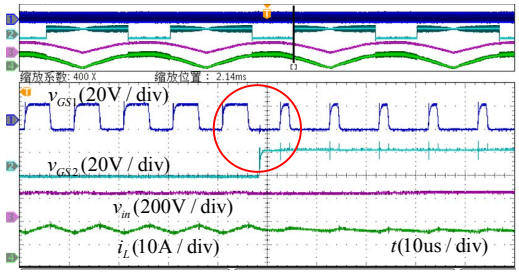

(b) Detail waveforms at the boundary of mode switching

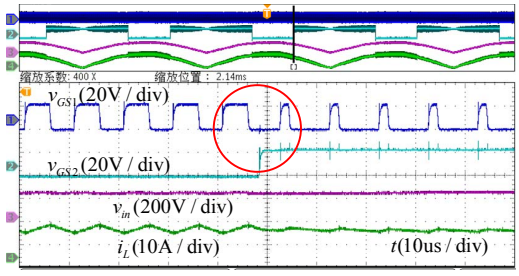

(c) Detail waveforms at the boundary of mode switching

Fig. 11. Steady state experimental waveforms v_{ac}=180VAC

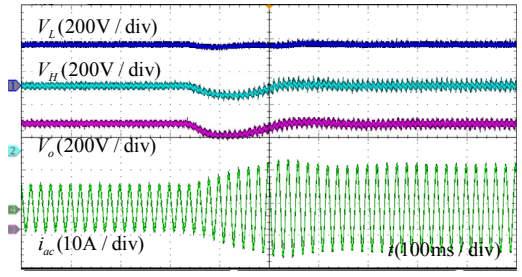

Fig. 12. Experimental waveforms of load stepping up

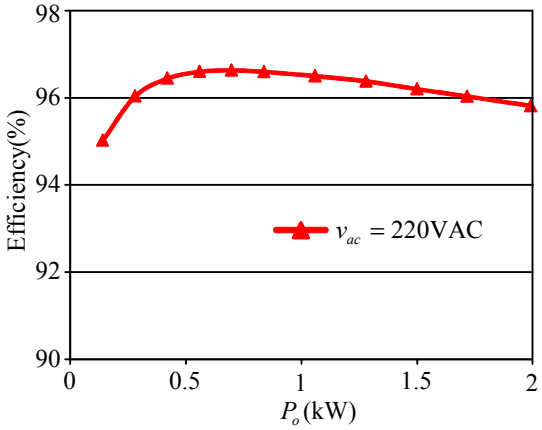

Fig. 13. Efficiency curve

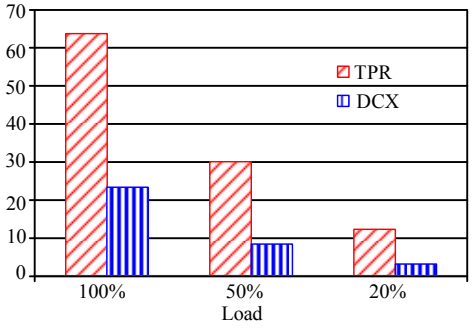

Fig. 14. Comparison of losses between the TPR and the DCX

only partial input power is processed by the high-efficiency DCX converter.

IV. Conclusions

A three-port Boost-rectifier-based single-phase PFC converter for high-efficiency and higher voltage application is analyzed which is composed of a three-port rectifier and an isolated DCX. The output of the DCX and the higher voltage port of the TPR are in series connection which can reduce the voltage stresses of the power devices. With the analyzed control scheme, the TPR can control the line current, the low voltage and the high voltage, simultaneously. Switching losses are reduced significantly since three voltage-levels can be generated by the TPR and only a power switch works at high frequency. Control technique based on the volt-second balance of the inductor is applied to the TPR and the transition of different working modes can be realized smoothly. Experimental results of a 2-kW prototype verify the effectiveness of the analyzed converter.

References

[1] H. Chen, C. Lu, C. Chen, "Current sensorless control for dual-Boost full-bridge PFC converter," IEEE APEC, 2017, pp.1-6.

[2] Y. Tang, W. Ding, A. Knaligh, "A bridgeless totem-pole interleaved PFC converter for plug-in electric vehicles," IEEE APEC, 2016, pp. 440-445.

[3] H Wu, M. Han, Y. Zhang, "Three-port rectifier-based AC-DC power converters with sigma architecture and reduced conversion stages," IEEE Journal of Emerging and Selected Topics in Power Electronics, vol. 5, no. 3, pp. 1091-1101, Sept 2017.

[4] G. Pandian, S. Rama Reddy, "Implementation of single phase to three phase PWM inverter fed induction motor drive," IET ICTES, 2007, pp. 355-360.

[5] B. Whitaker, A. Barkley, Z. Cole, et al, "A high-density, high-efficiency, isolated on-board vehicle battery charger utilizing silicon carbide power devices," IEEE Trans. Power Electronics, vol. 29, no. 5, pp. 2606-2617, May 2014.

[6] CY. Oh, DH. Kim, DG. Woo, WY. Sung, YS. Kim, BK. Lee, "A high-efficient nonisolated single-stage on-board battery charger for electric vehicles," IEEE Trans. on Power Electronics, vol. 28, no.12, pp. 5746-5757, Dec 2013.

[7] F Musavi, M Edington, W Eberle, WG Dunford, "Evaluation and efficiency comparison of front end AC-DC plug-in hybrid charger topologies," IEEE Trans on Smart Grid, vol. 3, no. 1, pp. 413-421, Oct 2011.

[8] MS Agamy, PK Jain, " An adaptive energy storage technique for efficiency improvement of single-stage three-level resonant AC/DC converters," IEEE APEC, 2009, pp. 1005-1010.

[9] A Kianpour, M Jabbari, G Shahgolian, "High step-up floating-output interleaved-input coupled-inductor-based boost converter," IEEE ICEE, 2016, pp. 1088-1093.

[10] HM Sizkoohi, J Milimonfared, M Taheri, S Salehi, "High step-up soft-switched dual-boost coupled-inductor-based converter integrating multipurpose coupled inductors with capacitor-diode stages," IEEE Trans on Power Electronics, vol. 8, no. 9, pp. 1786-1797, Mar 2015.

[11] J. C. Salmon, "Circuit topologies for single-phase voltage-doubler boost rectifers," IEEE APEC, 1992, pp. 549-556.

[12] D Maksimovic, R Erickson, "Universal-input, high-power-factor, boost doubler rectifiers," IEEE APEC, 1995, pp. 349-335.

[13] H Vahedi, PA Labbe, K Al-Haddad, "Single-Phase Single-Switch Vienna Rectifier as Electric Vehicle PFC Battery Charger," IEEE VPPC, 2015, pp. 1-6.